Atmos. Chem. Phys. Discuss., https://doi.org/10.5194/acp-2017-1008
Manuscript under review for journal Atmos. Chem. Phys.
Discussion started: 8 November 2017


Atmospheric Chemistry and Physics Discussions

# Comparison of secondary organic aerosol formation from toluene on initially wet and dry ammonium sulfate particles

Tengyu Liu[1], Dan Dan Huang[1], Zijun Li[2], Qianyun Liu[3], ManNin Chan[2,4], and Chak K. Chan[1,*]

1. School of Energy and Environment, City University of Hong Kong, Hong Kong, China
2. Earth System Science Programme, The Chinese University of Hong Kong, Hong Kong, China
3. Division of Environment and Sustainability, Hong Kong University of Science and Technology, Hong Kong, China
4. The Institute of Environment, Energy and Sustainability, The Chinese University of Hong Kong, Hong Kong, China

*Corresponding author:
Chak K. Chan
School of Energy and Environment, City University of Hong Kong, China
Tel: +852-34425593
Email: Chak.K.Chan@cityu.edu.hk

Atmos. Chem. Phys. Discuss., https://doi.org/10.5194/acp-2017-1008
Manuscript under review for journal Atmos. Chem. Phys.
Discussion started: 8 November 2017


Atmospheric Chemistry and Physics Discussions


## Abstract

The formation of secondary organic aerosol (SOA) has been widely studied in the presence of dry seed particles at low relative humidity (RH). At higher RH, seed particles can exist as dry or wet particles. Here, we investigated the formation of SOA from the photooxidation of toluene using an oxidation flow reactor under a range of OH exposures on initially wet or dry ammonium sulfate (AS) seed particles at an RH of 68%. At an OH exposure of $4.66\times10^{10}$ molecules $cm^{-3}$ s, the ratio of the SOA yield on wet AS seeds to that on dry AS seeds was 1.31±0.02. However, this ratio decreased to 1.01±0.01 at an OH exposure of $5.28\times10^{11}$ molecules $cm^{-3}$ s. The decrease in the ratios of SOA yields as the increase of OH exposure may be due to the early deliquescence of initially dry AS seeds after coated by highly oxidized toluene-derived SOA. SOA formation lowered the deliquescence RH of AS and resulted in the uptake of water by both AS and SOA. Hence the initially dry AS seeds contained aerosol liquid water (ALW) soon after a large fraction of SOA formed and the SOA yield and ALW approached those of the initially wet AS seeds as OH exposure and ALW increased. However, a higher oxidation state of the SOA on initially wet AS seeds than that on dry AS seeds was observed at all levels of OH exposure. The difference in mass fractions of *m/z* 29, 43 and 44 of SOA mass spectra indicated that SOA formed on initially wet seeds may be enriched in earlier-generation products containing carbonyl functional groups at low OH exposures and later-generation products containing acidic functional groups at high exposures. Our results suggest that AS dry seeds soon turn to at least partially deliquesced particles during SOA formation and more studies on the interplay

Atmos. Chem. Phys. Discuss., https://doi.org/10.5194/acp-2017-1008
Manuscript under review for journal Atmos. Chem. Phys.
Discussion started: 8 November 2017


Atmospheric Chemistry and Physics Discussions

of SOA formation and ALW are warranted.

Atmos. Chem. Phys. Discuss., https://doi.org/10.5194/acp-2017-1008
Manuscript under review for journal Atmos. Chem. Phys.
Discussion started: 8 November 2017


Atmospheric Chemistry and Physics Discussions

## 1. Introduction

Secondary organic aerosol (SOA) is an important component of atmospheric particulate matter, which influences air quality, climate and human health (Hallquist et al., 2009). SOA is mainly formed via the oxidation of volatile organic compounds (VOCs), followed by partitioning to the condensed phase. Traditional atmospheric chemical transport models largely underestimate the levels of SOA (de Gouw et al., 2005; Volkamer et al., 2006; Hodzic et al., 2010) and the degree of oxidation (Rudich et al., 2007; Ng et al., 2010). SOA yields in traditional atmospheric chemical transport models are obtained from smog chamber experiments using dry seed particles (Barsanti et al., 2013; Mahmud and Barsanti, 2013) under dry conditions. Yet, atmospheric relative humidity is often sufficiently high that aerosols often exist as wet aerosols, containing a large amount of aerosol liquid water (ALW) (Liao and Seinfeld, 2005; Lee and Adams, 2010; Guo et al., 2015; Nguyen et al., 2016). The presence of ALW in wet aerosols may enhance SOA formation by facilitating the partitioning of semivolatile organic compounds and the uptake of water-soluble gases through aqueous-phase reactions (Hennigan et al., 2008; Lim et al., 2010; Ervens et al., 2011; Lee et al., 2011; Sareen et al., 2017). ALW may also promote photodegradation of dissolved SOA (Romonosky et al., 2014). Therefore, SOA formation under atmospherically relevant relative humidity needs to be better constrained in atmospheric chemical transport models.

Aromatic hydrocarbons constitute a large fraction of the total non-methane hydrocarbons in the urban atmosphere (Calvert et al., 2002) and account for a significant fraction of SOA in urban areas (Ding et al., 2012; Zhao et al., 2017). Toluene



is the most abundant aromatic hydrocarbon (Calvert et al., 2002; Zhang et al., 2016) and SOA yields from the photooxidation of toluene on dry or wet ammonium sulfate (AS) seeds has been studied by varying the RH in smog chambers. Kamens et al. (2011) observed higher yields of SOA from toluene at higher RHs. They attributed this increase to the initially wet seed particles. On the other hand, Edney et al. (2000) reported that wet seeds had no effect on the SOA yields of toluene compared with dry seeds. In these studies, different RHs used for dry and wet seeds experiments may influence the gas-phase chemistry and complicate the comparison of SOA formation.

SOA formation on initially dry and wet AS seeds has been compared using oxidation flow reactors at same RHs (Wong et al., 2015; Faust et al., 2017). Faust et al. (2017) found a 19% enhancement in the SOA yield of toluene on wet AS seeds over that on dry AS seeds at 70% RH. However, at such high RH, the initially dry and water-free AS seed particles can uptake water upon SOA formation because SOA themselves can be hygroscopic and they can also lower the deliquescence RH of the AS seeds (Takahama et al., 2007; Smith et al., 2011, 2012, 2013). The potential influence of SOA formation on the physical state of the initially dry seeds as well as and the overall water uptake by the aged particles was not explicitly discussed. In addition, the hydroxyl radicals (OH) exposure in their study was approximately $2\times10^{11}$ molecules $cm^{-3}$ s, equivalent to about 1.5 days of oxidation in the atmosphere assuming an ambient OH concentration of $1.5\times10^{6}$ molecules $cm^{-3}$ (Mao et al., 2009). Atmospheric particles can undergo oxidation for as long as 1-2 weeks (Balkanski et al., 1993).

In this study, SOA formation from the photooxidation of toluene was investigated

Atmos. Chem. Phys. Discuss., https://doi.org/10.5194/acp-2017-1008
Manuscript under review for journal Atmos. Chem. Phys.
Discussion started: 8 November 2017




in an oxidation flow reactor at an RH of 68% under a wide range of OH exposures using initially wet or dry AS seed particles. The yields and composition of SOA as well as the estimated ALW contents for the initially wet and dry seeds are compared. We found that as OH exposure increased, the SOA yield and ALW of the initially dry seeds approached those of the initially wet seeds while the wet seeds yielded SOA of a higher degree of oxidation than the dry seeds did at all exposure levels.

## 2. Materials and methods

### 2.1 Generation of seed particles

A schematic of the experimental setup is shown in Fig. 1. AS seed particles were generated from an aqueous AS solution (Sigma-Aldrich) using an atomizer (TSI 3076, TSI Inc., USA). In experiments using dry seeds, the atomized aqueous AS droplets passed through a silica gel diffusion dryer so that the RH was reduced to less than 30% at which AS effloresced, while in experiments using wet seeds, they bypassed the diffusion dryer. The dry or wet seed particles then entered and mixed with a humidified $N_2/O_2/O_3$ flow in an oxidation flow reactor. The RH in the flow reactor was at 68%, which lies between the efflorescence and deliquescence RH of AS (Seinfeld and Pandis, 2006), so that the seed particles remained in their original phase with the wet particles containing ~18.6 μg $m^{-3}$ ALW and the dry particles anhydrous before reaction started. Hereafter, the experiments using initially wet and dry AS seed particles are simplified as wet and dry AS seeds, respectively. “Wet” and “dry” refer to the initial state of the seed particles before SOA formation.

When atomizing a given AS solution, the diameter of wet AS droplets is much



larger than that of dry AS particles due to the water uptake of AS (Chan et al., 1992), resulting in a larger surface area of seed particles. Previous studies have demonstrated that a large surface area of seed particles may increase the SOA yields by reducing the wall loss of organic vapors (Matsunaga and Ziemman, 2010, Zhang et al., 2014, 2015; Huang et al., 2016; Krechmer et al., 2016). To obtain seed particles of comparable surface areas, we atomized 0.013 mM and 0.015 mM of the AS solution for wet and dry AS seeds, respectively. As shown in Fig. S1, the surface area distribution of wet AS seeds was similar to that of dry AS seeds. Because of the difference in AS concentration between the stock solutions used, wet AS seeds had a mean diameter of 88 nm and were slightly smaller than dry AS seeds which had a mean diameter of 102 nm. The total surface area of wet AS seeds was 21% larger than that of dry AS seeds. The mass loading of wet and dry AS seeds was 31.0 and 24.2 μg $m^{-3}$, respectively.

**2.2 Oxidation flow reactor**

SOA formation from the photooxidation of toluene on initially dry or wet seeds was investigated in a potential aerosol mass (PAM) oxidation flow reactor, which has been described in detail elsewhere (Kang et al., 2007, 2011; Lambe et al., 2011a, 2015; Liu et al., 2017). Briefly, a PAM chamber is a continuous oxidation flow reactor using high and controlled levels of oxidants to oxidize gaseous precursors to produce SOA. The chamber used in this study had a volume of approximately 19 L (length 60 cm, diameter 20 cm). The total flow rate in the PAM chamber was set at 3 L $min^{-1}$ using mass flow controllers, resulting in a residence time of approximately 380 s. The RH and temperature of the PAM outflow were measured continuously (HMP 110, Vaisala Inc,



Finland) and stabilized at approximately 68% and 20 ºC, respectively. High OH exposures were realized through the photolysis of ozone irradiated by a UV lamp (λ = 254 nm) in the presence of water vapor. Ozone was produced by an ozone generator (1000BT-12, ENALY, Japan) via the irradiation of pure $O_2$. The OH concentration was adjusted by varying the concentration of ozone in the PAM chamber from 0.4 ppm to 4.3 ppm. The corresponding upper limit of OH exposure at these operating conditions ranged from $4.66\times10^{10}$ molecules $cm^{-3}$ s to $5.28\times10^{11}$ molecules $cm^{-3}$ s, equivalent to 0.36 to 4.08 days of atmospheric oxidation assuming an ambient OH concentration of $1.5\times10^{6}$ molecules $cm^{-3}$ (Mao et al., 2009). The addition of toluene may reduce the OH exposure. The upper limit of OH exposure was determined by measuring the decay of $SO_2$ (Model T100, TAPI Inc., USA) in the absence of toluene, following procedures described elsewhere (Kang et al., 2007; Lambe et al., 2011a). Peng et al. (2016) found that non-OH chemistry, including photolysis at λ = 254 nm and reactions with $O(^1D)$, $O(^3P)$ and $O_3$, may play an important role in oxidation flow reactors. In this study, the PAM reactor was operated at water vapor mixing ratios above 0.5% and external OH reactivity below 20 $s^{-1}$. Non-OH chemistry is expected to play a negligible role under these conditions (Peng et al., 2016).

Before and after each experiment, the PAM reactor was cleaned under an OH exposure of ~$1\times10^{12}$ molecules $cm^{-3}$ s until the mass concentration of background particles dropped below 3 μg $m^{-3}$. After characterizing dry or wet AS seed particles for half an hour, the UV lamp was turned on to oxidize the background gases at five different OH levels to measure the concentrations of background organics. A toluene



mixture (29.6 ppm in nitrogen) with a flow rate of 0.013 L $min^{-1}$ was then introduced to initiate SOA formation. The initial concentration of toluene in the PAM reactor was approximately 138 ppb. SOA was measured for at least an hour at each of the five OH levels.

**2.3 Characterization of non-refractory components**

The AS/SOA mixed particles were characterized for the chemical composition of non-refractory components including organics, sulfate and ammonium as well as the elemental ratios of organics using a high-resolution time-of-flight aerosol mass spectrometer (hereafter AMS, Aerodyne Research Incorporated, USA) (DeCarlo et al., 2006). The instrument was operated in the high sensitivity V-mode and the high resolution W-mode alternating every one minute. The toolkit Squirrel 1.57I and Pika 1.16I were used to analyze the AMS data. The molar ratios of hydrogen to carbon (H:C) and oxygen to carbon (O:C) were determined using the Aiken method (Aiken et al., 2007, 2008). The ionization efficiency of the AMS was calibrated using 300 nm ammonium nitrate particles. The particle-free matrix air, obtained by passing the air flow from the PAM reactor through a HEPA filter, was measured for at least 20 min before each experiment to determine the signals from major gases.

The collection efficiency (CE) of an AMS is dependent on the chemical composition and acidity as well as the phase state of particles (Matthew et al., 2008; Middlebrook et al., 2012). Matthew et al. (2008) found that the CE for solid particles thickly coated with liquid organics was 100%. In this study, experiments were conducted at an RH of 68%, exceeding the RH threshold for the semisolid-to-liquid



phase transition for toluene-derived SOA (Bateman et al., 2015; Song et al., 2016). A CE of 1 was used for processing all AMS data since the concentration of sulfate measured with the AMS varied by less than 5% of the average mass of sulfate after coated by SOA for both wet and dry AS seeds conditions. For the quantification of SOA, the contribution from background organic aerosols was subtracted from the total organic aerosols. The ratio of SOA mass to background organic mass ranged from 7 to 59, indicating that the contribution from background organics was negligible. Aerosol particles typically pass through a silica gel diffusion dryer to remove ALW before they are measured by AMS. However, this may lead to some losses of semivolatile organics through reversible partitioning (Wong et al., 2015; Faust et al., 2016). In this study, the AS/SOA mixed particles stream passed through and bypassed a diffusion dryer alternately before they were measured by AMS. Overall less than 8% of SOA were lost for wet and dry AS seeds after passing the diffusion dryer (Fig. S2), possibly due to reversible partitioning of the SVOCs. In this paper, the data reported are those bypassing the diffusion dryer.

A scanning mobility particle sizer (SMPS, TSI Incorporated, USA, classifier model 3082, CPC model 3775) was used to measure particle number concentrations and size distributions. Particle size ranged from 15 nm to 661 nm.

To evaluate the influence of seed surface area on SOA formation, we conducted another experiment at OH exposure of $4.66\times10^{10}$ molecules $cm^{-3}$ s with 50% of the seed surface area used in the wet AS experiment. The difference in SOA concentration was approximately 1% between these two experiments. Hence the 20% difference in seed

Atmos. Chem. Phys. Discuss., https://doi.org/10.5194/acp-2017-1008
Manuscript under review for journal Atmos. Chem. Phys.
Discussion started: 8 November 2017


Atmospheric Chemistry and Physics Discussions

surface area as well as the difference in mass loadings between wet and dry AS particles cannot account for the difference in SOA yield to be discussed below.

**2.4 Estimation of aerosol liquid water (ALW) content**

The ALW content of the initially dry AS was zero. However, as reactions proceed, SOA themselves can uptake water and also lower the deliquescence RH of AS, leading to water uptake by AS and some fractions of AS in aqueous phase. The ALW contents of AS ($ALW_{AS}$) and toluene-derived SOA ($ALW_{SOA}$) were estimated from the following equations (Kreidenweis et al., 2008):

$$ALW_{AS} = V_{AS}\kappa_{AS} f \frac{\alpha_w}{1-\alpha_w}\rho_w \quad (1)$$

$$ALW_{SOA} = V_{SOA}\kappa_{SOA} \frac{\alpha_w}{1-\alpha_w}\rho_w \quad (2)$$

where $V_{AS}$ and $V_{SOA}$ represent the volume concentrations of dry AS and SOA particles, $\kappa_{AS}$ is the hygroscopicity parameter of AS particles obtained from Kreidenweis et al. (2008), $\kappa_{SOA}$ is the hygroscopicity parameter of toluene-derived SOA calculated using the linear correlation between $\kappa_{SOA}$ and the O:C ratios of SOA proposed by Lambe et al. (2011b), the term $f$ is the fraction of AS particles that dissolved, $\alpha_w$ is the water activity and $\rho_w$ is the density of water (1.0 g $cm^{-3}$). Here, $\alpha_w$ was assumed to be equivalent to RH/100 for simplicity. The volume concentrations of dry AS and SOA particles were estimated from the measured mass concentration of AS and SOA assuming their respective particle densities to be 1.77 g $cm^{-3}$ and 1.4 g $cm^{-3}$ (Ng et al., 2007).

For the initially wet AS seeds, all AS particles were completely aqueous and therefore $f$ = 1. For the initially dry AS seeds, before reactions, the AS particles were

Atmos. Chem. Phys. Discuss., https://doi.org/10.5194/acp-2017-1008
Manuscript under review for journal Atmos. Chem. Phys.
Discussion started: 8 November 2017




completely dry and $f = 0$. After reactions, the AS particles became partially or entirely deliquesced upon the formation of toluene-derived SOA. The dissolved fraction of AS particles was regulated by the liquidus curve of the deliquescence relative humidity (DRH($\varepsilon$)) of AS particles coated with toluene-derived SOA (Smith et al., 2013):

$$f = \begin{cases} \dfrac{\varepsilon(1-\varepsilon_D)}{\varepsilon_D(1-\varepsilon)} & for\ \varepsilon < \varepsilon_D \\ 1 \quad for \quad \varepsilon \geq \varepsilon_D \end{cases} \tag{3}$$

The term $\varepsilon$ is the volume fraction of SOA. The term $\varepsilon_D$, representing the volume fraction of organics at which the mixture of SOA and AS particles deliquesced at an RH of 68%, was estimated to be 0.75 based on the liquidus curve.

## 3. Results and discussion

### 3.1 SOA yields

Figure 2a shows SOA yields from the photooxidation of toluene on initially wet and dry AS seed particles as a function of OH exposure. The SOA yield was calculated as the SOA mass divided by the mass of reacted toluene. The mass of reacted toluene was calculated from the OH exposure and the rate constant of the reaction between toluene and OH (Atkinson and Arey, 2003). The uncertainty in the SOA yields fully reflected the uncertainty in the calculation of the SOA mass. In both cases, SOA yields first exhibited an increase, followed by a decrease as the level of OH exposure increased. This trend may be due to the transition of functionalization reactions to fragmentation ones (Kroll et al., 2009; Lambe et al., 2011a). The SOA yields for dry and wet AS seeds were 0.18–0.31 and 0.22–0.36, respectively, significantly higher than the value of 0.0059 observed in an oxidation flow reactor under comparable conditions (Faust et al.,



238 2017) and the value of 0.09 obtained in another PAM chamber at 30% RH in the
239 absence of seed particles (Kang et al., 2007). Faust et al. (2017) attributed their
240 significantly lower yields than typical literature values of 0.09–0.30 (Lambe et al.,
241 2011a; Ng et al., 2007) to the wall loss of particles and the fragmentation of organics in
242 their flow reactor. On the other hand, the SOA yields we obtained are lower than 0.30–
243 0.37 from smog chamber experiments conducted at a similar temperature, SOA mass
244 loading and OH exposure but a lower RH with dry AS seeds (Ng et al., 2007;
245 Hildebrandt et al., 2009). Note that the wall loss of particles was not corrected in this
246 study, so the SOA yields may be underestimated. As wet and dry AS seeds in this study
247 had similar particle number size distributions, the wall loss of particles would not affect
248 the comparison of SOA yield between wet and dry AS seeds.

249 As shown in Fig. 2a, a higher SOA yield was observed for wet AS seeds than for
250 dry AS seeds at the same OH exposure and the difference in SOA yield decreased as
251 the OH exposure increased. The ratio of SOA yields on wet AS seeds to those on dry
252 AS seeds was 1.31±0.02 at an OH exposure of $4.66\times10^{10}$ molecules $cm^{-3}$ s but
253 decreased to 1.01±0.01 when the OH exposure was increased to $5.28\times10^{11}$ molecules
254 $cm^{-3}$ s (Fig. 2b). These ratios are comparable to the 1.19±0.05 observed by Faust et al.
255 (2017) at an OH exposure of approximately $2.0\times10^{11}$ molecules $cm^{-3}$ s.

256 The formation of SOA on initially dry AS particles may alter the deliquescence
257 relative humidity (DRH) of AS particles. Smith et al. (2013) found that when coated
258 with toluene-derived SOA, the DRH of AS particles decreased from 80% to 58% as the
259 organic volume fraction increased from 0 to 0.8. Therefore, coating AS particles with



toluene-derived SOA can change the physical state of initially dry AS seeds and increase the content of $ALW_{AS,\ dry}$. As shown in Fig. 3a, after reactions, the mass concentrations of $ALW_{tot}$ (= $ALW_{SOA}$ + $ALW_{AS}$) and $ALW_{SOA}$ increased for both wet and dry seeds as the OH exposure increased. The uncertainties for $ALW_{SOA}$ and $ALW_{AS}$ were 22% and less than 3%, respectively. They reflect the uncertainties in κ and volume concentrations of AS and SOA. The increase in $ALW_{tot,\ wet}$ was due to the increase in $ALW_{SOA,\ wet}$ while the increase in $ALW_{tot,\ dry}$ was driven by the increase in $ALW_{AS,\ dry}$ at lower OH exposure and by $ALW_{SOA,\ dry}$ at higher OH exposures. At OH exposure of $4.66\times10^{10}$ molecules $cm^{-3}$ s, $ALW_{AS,\ dry}$ increased from 0 to 6.2 μg $m^{-3}$ after reactions due to the partial deliquescence ($f$=0.43) of the originally dry AS particles after SOA formation. The difference in $ALW_{AS,\ dry}$ and $ALW_{AS,\ wet}$ narrowed and the $ALW_{total}$ of initially dry AS seeds partially resembled those of the wet ones. At OH exposure between $1.66\times10^{11}$ and $5.28\times10^{11}$ molecules $cm^{-3}$ s, the total final organic volume fraction increased to approximately 0.8 and the initially dry AS particles entirely deliquesced after reactions. Based on the reported SOA yield, initial toluene concentration, OH exposure and assumed concentrations of AS seeds (~10-40 μg $m^{-3}$) in Faust et al. (2017), we estimated that an upper limit of 48% of the initially dry AS seeds has deliquesced in their study. Similar to this study, SOA coatings on seed particles may change the physical state of initially dry seeds and lower the difference of SOA yields between initially dry and wet seeds experiments.

### 3.2 Chemical composition of SOA

Atmos. Chem. Phys. Discuss., https://doi.org/10.5194/acp-2017-1008
Manuscript under review for journal Atmos. Chem. Phys.
Discussion started: 8 November 2017




Figure 4 shows the high-resolution mass spectra of SOA for initially wet and dry AS seeds at OH exposures of $4.66\times10^{10}$ molecules $cm^{-3}$ s and $5.28\times10^{11}$ molecules $cm^{-3}$ s. For both types of AS seeds, at an OH exposure of $4.66\times10^{10}$ molecules $cm^{-3}$ s, the most prominent peaks were *m/z* 29 and 43, followed by *m/z* 28 and 44. *m/z* 29 was dominated by ion $CHO^+$, a tracer for alcohols and aldehydes (Lee et al., 2012). The *m/z* 28 and *m/z* 44 signals, respectively dominated by $CO^+$ and $CO_2^+$, are tracers for organic acids (Ng et al., 2010). At the OH exposure of $5.28\times10^{11}$ molecules $cm^{-3}$ s, the dominant peaks were *m/z* 28 and 44, followed by *m/z* 29 and 43. The increase of mass fractions of the oxygen-containing ions in the SOA mass spectra at a relatively high OH exposure suggests the formation of more oxidized organic aerosols. Furthermore, ions with *m/z* > 80 accounted for a negligible fraction of total SOA, suggesting that oligomerization might not be important in these experiments. On the basis of the mass fraction of ions, Fig. S3 shows that as OH exposure increased, the difference (wet minus dry) in the spectra of toluene-derived SOA changed from positive in *m/z* 29 ($CHO^+$) and *m/z* 43 ($C_2H_3O^+$) to *m/z* 28 ($CO^+$) and *m/z* 44 ($CO_2^+$). The increase in OH exposure resulted in a change from more alcohols or aldehydes to more organic acids in the wet seeded case when compared to the dry seeded case.

Fragments derived from the AMS data have been extensively used to infer the bulk compositions and evolution of organic aerosols (Zhang et al., 2005; Ng et al., 2010; Heald et al., 2010). Here we used the approach of Ng et al. (2010) and plotted the fractions of the total organic signal at *m/z* 43 ($f_{43}$) vs. *m/z* 44 ($f_{44}$) as well as the triangle based on the analysis of ambient AMS data (Fig. 5). Ng et al. (2010) proposed that



aging would cause $f_{43}$ and $f_{44}$ to converge toward the triangle apex ($f_{43}$ = 0.02, $f_{44}$ = 0.30). For both wet and dry AS seeds, $f_{43}$ first increased and then decreased with the increase of OH exposure, while $f_{44}$ increased all the time. This reversing trend of $f_{43}$ was the result of the increase and subsequent decrease in $C_2H_3O^+$ (Fig. S4), an indicator of products containing carbonyl functional groups. It was also observed for SOA formed from other precursors such as alkanes and naphthalene (Lambe et al., 2011b). Before the decrease in $f_{43}$, SOA formed on wet AS seeds had higher $f_{43}$ and similar $f_{44}$ to SOA formed on dry AS seeds at the same OH exposure. As OH exposure increased, SOA formed on wet AS seeds had higher $f_{44}$ and lower $f_{43}$ than SOA formed on dry AS seeds. The $f_{43}$-$f_{44}$ plot supports our earlier assertion that as OH exposure increased, the reaction products changed from earlier-generation products containing carbonyl functional groups to later-generation products containing acidic functional groups. In addition, as OH exposure increased, SOA formed on wet AS seeds initially had more earlier-generation products but later had more acidic later-generation products than SOA formed on dry AS seeds, likely due to the enhanced partitioning of these products on initially wet AS seeds and/or enhanced uptake of water-soluble gases through aqueous phase reactions.

Figure 6 shows the changes in H:C and O:C ratios as a function of OH exposure in a Van Krevelen diagram (Heald et al., 2010). The standard deviations for H:C and O:C values were both less than 0.01. The O:C ratios for dry and wet AS seeds were in the ranges of 0.59–0.89 and 0.63–0.95, respectively. At the same OH exposure, SOA on wet AS seeds had both higher O:C ratios and estimated average carbon oxidation state



325 ($OS_C$) ($OS_C \approx 2\times O{:}C - H{:}C$) (Kroll et al., 2011) than dry AS seeds had. Fig. 6 also
326 shows some of the identified SOA products from the photoxidation of toluene (Bloss et
327 al., 2005; Hamilton et al., 2005; Sato et al., 2007). The elevated $OS_c$ (exceeding 0.5)
328 could only be due to the formation of highly oxgenerated small acids such as pyruvic
329 acid ($OS_C$ = 0.67), glycolic acid ($OS_C$ = 1), formic acid ($OS_C$ = 2), oxalic acid ($OS_C$ =
330 3), malonic acid ($OS_C$ = 1.33) and glyoxylic acid ($OS_C$ = 2). Small acids may be
331 important products of toluene-derived SOA at high OH exposures. Fisseha et al. (2004)
332 found that small organic acids accounted for 20–45% of SOA from the photooxidation
333 of 1,3,5-trimethylbenzene. The higher $OS_c$ at high OH exposures for wet AS seeds
334 might suggest that these small acids were more abundant, likely due to their enhanced
335 retention in the presence of ALW and/or the more efficient uptake of OH radicals by
336 wet AS seeds and further oxidation reactions in aqueous phase (Ruehl et al., 2013). The
337 change in the slope of H:C vs O:C is consistent with the earlier analysis that the
338 mechanism of SOA formation changed from functionalization dominated by the
339 addition of alcohol/peroxide (Heald et al., 2010; Ng et al., 2011) at low exposures to
340 the addition of both acid and alcohol/peroxide functional groups without fragmentation,
341 and/or the addition of acid groups with fragmentation at high exposures.

342 **3.3 Atmospheric implications**

343 In this work, yields and composition of SOA formed from the photooxidation of toluene
344 on initially wet and dry AS seeds were compared over a wide range of OH exposures,
345 covering the transition from functionalization reactions to fragmentation reactions. We
346 found that the ratio of SOA yield on wet AS seeds to that on dry AS seeds decreased



347 from 1.31 to 1.01 as the OH exposure increased from $4.66\times10^{10}$ to $5.28\times10^{11}$ molecules
348 $cm^{-3}$ s. This decrease coincides with the decrease of differences in ALW between the
349 wet and dry cases, which may be due to water uptake by SOA as well as the early
350 deliquescence of dry AS particles as a result of SOA formation.

351 In addition to relatively higher SOA yields, higher O:C and $OS_c$ of SOA derived
352 from the photooxidation of toluene were also observed on initially wet AS seeds.
353 Particularly, the O:C in the presence of initially wet AS seeds could be as high as 0.95.
354 Chen et al. (2015) observed large gaps between laboratory and ambient measured O:C
355 of OA and suggested that OA having a high O:C (> 0.6) was required to bridge these
356 gaps. The multiphase oxidation of toluene in the presence of wet aerosols may be a
357 pathway to contribute to this gap. However, the relative importance of such chemistry
358 to the evolution of ambient OA remains unclear.

359 Our results suggest that dry seeds would quickly turn to at least partially
360 deliquesced particles upon SOA formation under moderate RH conditions. Since
361 ambient RH is rarely at such low values that inorganic particles remain dry even after
362 SOA formation, more laboratory and field studies are needed to elucidate the formation
363 and evolution of OA in wet aerosols.

**Acknowledgments**

The work described in this paper was sponsored by the Science Technology and Innovation Committee of Shenzhen Municipality (project no. JCYJ20160401095857424). Zijun Li and ManNin Chan are supported by a Direct Grant for Research (4053159), The Chinese University of Hong Kong and a Research Grants Council grant (RGC 2191111). Chak K. Chan would like to thank the Hong Kong University of Science and Technology for the use of the AMS.



## References

Aiken, A. C., DeCarlo, P. F., and Jimenez, J. L.: Elemental Analysis of Organic Species with Electron Ionization High-Resolution Mass Spectrometry, Anal. Chem., 79, 8350-8358, https://doi.org/10.1021/ac071150w, 2007.

Aiken, A. C., DeCarlo, P. F., Kroll, J. H., Worsnop, D. R., Huffman, J. A., Docherty, K. S., Ulbrich, I. M., Mohr, C., Kimmel, J. R., Sueper, D., Sun, Y., Zhang, Q., Trimborn, A., Northway, M., Ziemann, P. J., Canagaratna, M. R., Onasch, T. B., Alfarra, M. R., Prevot, A. S. H., Dommen, J., Duplissy, J., Metzger, A., Baltensperger, U., and Jimenez, J. L.: O/C and OM/OC Ratios of Primary, Secondary, and Ambient Organic Aerosols with High-Resolution Time-of-Flight Aerosol Mass Spectrometry, Environ. Sci. Technol., 42, 4478-4485, https://doi.org/10.1021/es703009q, 2008.

Atkinson, R., and Arey, J.: Atmospheric Degradation of Volatile Organic Compounds, Chem. Rev., 103, 4605-4638, https://doi.org/10.1021/cr0206420, 2003.

Balkanski, Y. J., Jacob, D. J., Gardner, G. M., Graustein, W. C., and Turekian, K. K.: Transport and residence times of tropospheric aerosols inferred from a global three-dimensional simulation of 210Pb, J. Geophys. Res.-Atmos., 98, 20573-20586, https://doi.org/10.1029/93JD02456, 1993.

Barsanti, K. C., Carlton, A. G., and Chung, S. H.: Analyzing experimental data and model parameters: implications for predictions of SOA using chemical transport models, Atmos. Chem. Phys., 13, 12073-12088, https://doi.org/10.5194/acp-13-12073-2013, 2013.

Bateman, A. P., Bertram, A. K., and Martin, S. T.: Hygroscopic Influence on the Semisolid-to-Liquid Transition of Secondary Organic Materials, J. Phys. Chem. A, 119, 4386-4395, https://doi.org/10.1021/jp508521c, 2015.

Bloss, C., Wagner, V., Jenkin, M. E., Volkamer, R., Bloss, W. J., Lee, J. D., Heard, D. E., Wirtz, K., Martin-Reviejo, M., Rea, G., Wenger, J. C., and Pilling, M. J.: Development of a detailed chemical mechanism (MCMv3.1) for the atmospheric oxidation of aromatic hydrocarbons, Atmos. Chem. Phys., 5, 641-664, https://doi.org/10.5194/acp-5-641-2005, 2005.

Calvert, J. G., Atkinson, R., Becker, K. H., Kamens, R. M., Seinfeld, J. H., Wallington, T. H., and Yarwood, G.: The Mechanisms of Atmospheric Oxidation of the Aromatic Hydrocarbons, Oxford University Press, New York, 556 pp., 2002.

Chen, Q., Heald, C. L., Jimenez, J. L., Canagaratna, M. R., Zhang, Q., He, L.-Y., Huang, X.-F., Campuzano-Jost, P., Palm, B. B., Poulain, L., Kuwata, M., Martin, S. T., Abbatt, J. P. D., Lee, A. K. Y., and Liggio, J.: Elemental composition of organic aerosol: The gap between ambient and laboratory measurements, Geophys. Res. Lett., 42, 2015GL063693, https://doi.org/10.1002/2015GL063693, 2015.

de Gouw, J. A., Middlebrook, A. M., Warneke, C., Goldan, P. D., Kuster, W. C., Roberts, J. M., Fehsenfeld, F. C., Worsnop, D. R., Canagaratna, M. R., Pszenny, A. A. P., Keene, W. C., Marchewka, M., Bertman, S. B., and Bates, T. S.: Budget of organic carbon in a polluted atmosphere: Results from the New England Air Quality Study in 2002, J. Geophys. Res.-Atmos., 110, D16305, https://doi.org/10.1029/2004JD005623, 2005.

DeCarlo, P. F., Kimmel, J. R., Trimborn, A., Northway, M. J., Jayne, J. T., Aiken, A. C., Gonin, M., Fuhrer, K., Horvath, T., Docherty, K. S., Worsnop, D. R., and Jimenez, J. L.: Field-Deployable, High-Resolution, Time-of-Flight Aerosol Mass Spectrometer, Anal. Chem., 78, 8281-8289, https://doi.org/10.1021/ac061249n, 2006.

Ding, X., Wang, X.-M., Gao, B., Fu, X.-X., He, Q.-F., Zhao, X.-Y., Yu, J.-Z., and Zheng, M.: Tracer-based estimation of secondary organic carbon in the Pearl River Delta, south China, J. Geophys. Res.-Atmos., 117, D05313, https://doi.org/10.1029/2011JD016596, 2012.

Edney, E. O., Driscoll, D. J., Speer, R. E., Weathers, W. S., Kleindienst, T. E., Li, W., and Smith, D. F.: Impact of aerosol liquid water on secondary organic aerosol yields of irradiated toluene/propylene/NOx/(NH4)2SO4/air mixtures, Atmos. Environ., 34, 3907-3919, 2000.

Ervens, B., Turpin, B. J., and Weber, R. J.: Secondary organic aerosol formation in cloud droplets and aqueous particles (aqSOA): a review of laboratory, field and model studies, Atmos. Chem. Phys., 11, 11069-11102, https://doi.org/10.5194/acp-11-11069-2011, 2011.

Faust, J. A., Wong, J. P. S., Lee, A. K. Y., and Abbatt, J. P. D.: Role of Aerosol Liquid Water in Secondary Organic Aerosol Formation from Volatile Organic Compounds, Environ. Sci. Technol., 51, 1405-1413, https://doi.org/10.1021/acs.est.6b04700, 2017.

Fisseha, R., Dommen, J., Sax, M., Paulsen, D., Kalberer, M., Maurer, R., Höfler, F., Weingartner, E., and Baltensperger, U.: Identification of Organic Acids in Secondary Organic Aerosol and the Corresponding Gas Phase from Chamber Experiments, Anal. Chem., 76, 6535-6540, https://doi.org/10.1021/ac048975f, 2004.

Guo, H., Xu, L., Bougiatioti, A., Cerully, K. M., Capps, S. L., Hite Jr, J. R., Carlton, A. G., Lee, S. H., Bergin, M. H., Ng, N. L., Nenes, A., and Weber, R. J.: Fine-particle water and pH in the southeastern United States, Atmos. Chem. Phys., 15, 5211-5228, https://doi.org/10.5194/acp-15-5211-2015, 2015.

Hallquist, M., Wenger, J. C., Baltensperger, U., Rudich, Y., Simpson, D., Claeys, M., Dommen, J., Donahue, N. M., George, C., Goldstein, A. H., Hamilton, J. F., Herrmann, H., Hoffmann, T., Iinuma, Y., Jang, M., Jenkin, M. E., Jimenez, J. L., Kiendler-Scharr, A., Maenhaut, W., McFiggans, G., Mentel, T. F., Monod, A., Prévôt, A. S. H., Seinfeld, J. H., Surratt, J. D., Szmigielski, R., and Wildt, J.: The formation, properties and impact of secondary organic aerosol: current and emerging issues, Atmos. Chem. Phys., 9, 5155-5236, https://doi.org/10.5194/acp-9-5155-2009, 2009.

Hamilton, J. F., Webb, P. J., Lewis, A. C., and Reviejo, M. M.: Quantifying small molecules in secondary organic aerosol formed during the photo-oxidation of toluene with hydroxyl radicals, Atmos. Environ., 39, 7263-7275, http://dx.doi.org/10.1016/j.atmosenv.2005.09.006, 2005.

Heald, C. L., Kroll, J. H., Jimenez, J. L., Docherty, K. S., DeCarlo, P. F., Aiken, A. C., Chen, Q., Martin, S. T., Farmer, D. K., and Artaxo, P.: A simplified description of the evolution of organic aerosol composition in the atmosphere, Geophys. Res. Lett., 37, L08803, https://doi.org/10.1029/2010gl042737, 2010.

457 Hennigan, C. J., Bergin, M. H., Dibb, J. E., and Weber, R. J.: Enhanced secondary organic
458 aerosol formation due to water uptake by fine particles, Geophys. Res. Lett., 35,
459 L18801, https://doi.org/10.1029/2008GL035046, 2008.
460 Hildebrandt, L., Donahue, N. M., and Pandis, S. N.: High formation of secondary organic
461 aerosol from the photo-oxidation of toluene, Atmos. Chem. Phys., 9, 2973-2986,
462 https://doi.org/10.5194/acp-9-2973-2009, 2009.
463 Hodzic, A., Jimenez, J. L., Madronich, S., Canagaratna, M. R., DeCarlo, P. F., Kleinman, L.,
464 and Fast, J.: Modeling organic aerosols in a megacity: potential contribution of semi-
465 volatile and intermediate volatility primary organic compounds to secondary organic
466 aerosol formation, Atmos. Chem. Phys., 10, 5491-5514, https://doi.org/10.5194/acp-
467 10-5491-2010, 2010.
468 Huang, D. D., Zhang, X., Dalleska, N. F., Lignell, H., Coggon, M. M., Chan, C.-M., Flagan,
469 R. C., Seinfeld, J. H., and Chan, C. K.: A note on the effects of inorganic seed aerosol
470 on the oxidation state of secondary organic aerosol—α-Pinene ozonolysis, J.
471 Geophys. Res.-Atmos., 121, 2016JD025999, https://doi.org/10.1002/2016JD025999,
472 2016.
473 Kamens, R. M., Zhang, H. F., Chen, E. H., Zhou, Y., Parikh, H. M., Wilson, R. L., Galloway,
474 K. E., and Rosen, E. P.: Secondary organic aerosol formation from toluene in an
475 atmospheric hydrocarbon mixture: Water and particle seed effects, Atmos. Environ.,
476 45, 2324-2334, https://doi.org/doi:10.1016/j.atmosenv.2010.11.007, 2011.
477 Kang, E., Root, M. J., Toohey, D. W., and Brune, W. H.: Introducing the concept of Potential
478 Aerosol Mass (PAM), Atmos. Chem. Phys., 7, 5727-5744,
479 https://doi.org/10.5194/acp-7-5727-2007, 2007.
480 Kang, E., Toohey, D. W., and Brune, W. H.: Dependence of SOA oxidation on organic
481 aerosol mass concentration and OH exposure: experimental PAM chamber studies,
482 Atmos. Chem. Phys., 11, 1837-1852, https://doi.org/10.5194/acp-11-1837-2011,
483 2011.
484 Krechmer, J. E., Pagonis, D., Ziemann, P. J., and Jimenez, J. L.: Quantification of Gas-Wall
485 Partitioning in Teflon Environmental Chambers Using Rapid Bursts of Low-
486 Volatility Oxidized Species Generated in Situ, Environ. Sci. Technol., 50, 5757-5765,
487 https://doi.org/10.1021/acs.est.6b00606, 2016.
488 Kreidenweis, S. M., Petters, M. D., and DeMott, P. J.: Single-parameter estimates of
489 aerosol water content, Environ. Res. Lett., 3, 035002, 2008.
490 Kroll, J. H., Smith, J. D., Che, D. L., Kessler, S. H., Worsnop, D. R., and Wilson, K. R.:
491 Measurement of fragmentation and functionalization pathways in the heterogeneous
492 oxidation of oxidized organic aerosol, Phys. Chem. Chem. Phys., 11, 8005-8014,
493 https://doi.org/10.1039/B905289E, 2009.
494 Kroll, J. H., Donahue, N. M., Jimenez, J. L., Kessler, S. H., Canagaratna, M. R., Wilson, K.
495 R., Altieri, K. E., Mazzoleni, L. R., Wozniak, A. S., Bluhm, H., Mysak, E. R., Smith,
496 J. D., Kolb, C. E., and Worsnop, D. R.: Carbon oxidation state as a metric for
497 describing the chemistry of atmospheric organic aerosol, Nat. Chem., 3, 133-139,
498 2011.
499 Lambe, A. T., Ahern, A. T., Williams, L. R., Slowik, J. G., Wong, J. P. S., Abbatt, J. P. D.,
500 Brune, W. H., Ng, N. L., Wright, J. P., Croasdale, D. R., Worsnop, D. R., Davidovits,

P., and Onasch, T. B.: Characterization of aerosol photooxidation flow reactors: heterogeneous oxidation, secondary organic aerosol formation and cloud condensation nuclei activity measurements, Atmos. Meas. Tech., 4, 445-461, https://doi.org/10.5194/amt-4-445-2011, 2011a.

Lambe, A. T., Onasch, T. B., Massoli, P., Croasdale, D. R., Wright, J. P., Ahern, A. T., Williams, L. R., Worsnop, D. R., Brune, W. H., and Davidovits, P.: Laboratory studies of the chemical composition and cloud condensation nuclei (CCN) activity of secondary organic aerosol (SOA) and oxidized primary organic aerosol (OPOA), Atmos. Chem. Phys., 11, 8913-8928, https://doi.org/10.5194/acp-11-8913-2011, 2011b.

Lambe, A. T., Chhabra, P. S., Onasch, T. B., Brune, W. H., Hunter, J. F., Kroll, J. H., Cummings, M. J., Brogan, J. F., Parmar, Y., Worsnop, D. R., Kolb, C. E., and Davidovits, P.: Effect of oxidant concentration, exposure time, and seed particles on secondary organic aerosol chemical composition and yield, Atmos. Chem. Phys., 15, 3063-3075, https://doi.org/10.5194/acp-15-3063-2015, 2015.

Lee, A. K. Y., Herckes, P., Leaitch, W. R., Macdonald, A. M., and Abbatt, J. P. D.: Aqueous OH oxidation of ambient organic aerosol and cloud water organics: Formation of highly oxidized products, Geophys. Res. Lett., 38, L11805, https://doi.org/10.1029/2011GL047439, 2011.

Lee, Y. H., and Adams, P. J.: Evaluation of aerosol distributions in the GISS-TOMAS global aerosol microphysics model with remote sensing observations, Atmos. Chem. Phys., 10, 2129-2144, https://doi.org/10.5194/acp-10-2129-2010, 2010.

Liao, H., and Seinfeld, J. H.: Global impacts of gas-phase chemistry-aerosol interactions on direct radiative forcing by anthropogenic aerosols and ozone, J. Geophys. Res.-Atmos., 110, D18208, https://doi.org/10.1029/2005JD005907, 2005.

Lim, Y. B., Tan, Y., Perri, M. J., Seitzinger, S. P., and Turpin, B. J.: Aqueous chemistry and its role in secondary organic aerosol (SOA) formation, Atmos. Chem. Phys., 10, 10521-10539, https://doi.org/10.5194/acp-10-10521-2010, 2010.

Liu, T., Li, Z., Chan, M., and Chan, C. K.: Formation of secondary organic aerosols from gas-phase emissions of heated cooking oils, Atmos. Chem. Phys., 17, 7333-7344, https://doi.org/10.5194/acp-17-7333-2017, 2017.

Mahmud, A., and Barsanti, K.: Improving the representation of secondary organic aerosol (SOA) in the MOZART-4 global chemical transport model, Geosci. Model Dev., 6, 961-980, 10.5194/gmd-6-961-2013, 2013.

Mao, J., Ren, X., Brune, W. H., Olson, J. R., Crawford, J. H., Fried, A., Huey, L. G., Cohen, R. C., Heikes, B., Singh, H. B., Blake, D. R., Sachse, G. W., Diskin, G. S., Hall, S. R., and Shetter, R. E.: Airborne measurement of OH reactivity during INTEX-B, Atmos. Chem. Phys., 9, 163-173, https://doi.org/10.5194/acp-9-163-2009, 2009.

Matsunaga, A., and Ziemann ‡, P. J.: Gas-Wall Partitioning of Organic Compounds in a Teflon Film Chamber and Potential Effects on Reaction Product and Aerosol Yield Measurements, Aerosol Sci. Tech., 44, 881-892, https://doi.org/10.1080/02786826.2010.501044, 2010.

Matthew, B. M., Middlebrook, A. M., and Onasch, T. B.: Collection Efficiencies in an Aerodyne Aerosol Mass Spectrometer as a Function of Particle Phase for Laboratory

Generated Aerosols, Aerosol Sci. Tech., 42, 884-898, https://doi.org/10.1080/02786820802356797, 2008.

Middlebrook, A. M., Bahreini, R., Jimenez, J. L., and Canagaratna, M. R.: Evaluation of Composition-Dependent Collection Efficiencies for the Aerodyne Aerosol Mass Spectrometer using Field Data, Aerosol Sci. Tech., 46, 258-271, https://doi.org/10.1080/02786826.2011.620041, 2012.

Ng, N. L., Kroll, J. H., Chan, A. W. H., Chhabra, P. S., Flagan, R. C., and Seinfeld, J. H.: Secondary organic aerosol formation from m-xylene, toluene, and benzene, Atmos. Chem. Phys., 7, 3909-3922, https://doi.org/10.5194/acp-7-3909-2007, 2007.

Ng, N. L., Canagaratna, M. R., Zhang, Q., Jimenez, J. L., Tian, J., Ulbrich, I. M., Kroll, J. H., Docherty, K. S., Chhabra, P. S., Bahreini, R., Murphy, S. M., Seinfeld, J. H., Hildebrandt, L., Donahue, N. M., DeCarlo, P. F., Lanz, V. A., Prévôt, A. S. H., Dinar, E., Rudich, Y., and Worsnop, D. R.: Organic aerosol components observed in Northern Hemispheric datasets from Aerosol Mass Spectrometry, Atmos. Chem. Phys., 10, 4625-4641, https://doi.org/10.5194/acp-10-4625-2010, 2010.

Ng, N. L., Canagaratna, M. R., Jimenez, J. L., Chhabra, P. S., Seinfeld, J. H., and Worsnop, D. R.: Changes in organic aerosol composition with aging inferred from aerosol mass spectra, Atmos. Chem. Phys., 11, 6465-6474, https://doi.org/10.5194/acp-11-6465-2011, 2011.

Nguyen, T. K. V., Zhang, Q., Jimenez, J. L., Pike, M., and Carlton, A. G.: Liquid Water: Ubiquitous Contributor to Aerosol Mass, Environ. Sci. Technol. Lett., 3, 257-263, https://doi.org/10.1021/acs.estlett.6b00167, 2016.

Parikh, H. M., Carlton, A. G., Vizuete, W., and Kamens, R. M.: Modeling secondary organic aerosol using a dynamic partitioning approach incorporating particle aqueous-phase chemistry, Atmos. Environ., 45, 1126-1137, http://dx.doi.org/10.1016/j.atmosenv.2010.11.027, 2011.

Peng, Z., Day, D. A., Ortega, A. M., Palm, B. B., Hu, W., Stark, H., Li, R., Tsigaridis, K., Brune, W. H., and Jimenez, J. L.: Non-OH chemistry in oxidation flow reactors for the study of atmospheric chemistry systematically examined by modeling, Atmos. Chem. Phys., 16, 4283-4305, https://doi.org/10.5194/acp-16-4283-2016, 2016.

Romonosky, D. E., Laskin, A., Laskin, J., and Nizkorodov, S. A.: High-Resolution Mass Spectrometry and Molecular Characterization of Aqueous Photochemistry Products of Common Types of Secondary Organic Aerosols, The Journal of Physical Chemistry A, 119, 2594-2606, https://doi.org/10.1021/jp509476r, 2015.

Rudich, Y., Donahue, N. M., and Mentel, T. F.: Aging of organic aerosol: Bridging the gap between laboratory and field studies, Annual Review of Physical Chemistry, 58, 321-352, https://doi.org/10.1146/annurev.physchem.58.032806.104432, 2007.

Ruehl, C. R., Nah, T., Isaacman, G., Worton, D. R., Chan, A. W. H., Kolesar, K. R., Cappa, C. D., Goldstein, A. H., and Wilson, K. R.: The Influence of Molecular Structure and Aerosol Phase on the Heterogeneous Oxidation of Normal and Branched Alkanes by OH, J. Phys. Chem. A, 117, 3990-4000, https://doi.org/10.1021/jp401888q, 2013.

Sareen, N., Waxman, E. M., Turpin, B. J., Volkamer, R., and Carlton, A. G.: Potential of Aerosol Liquid Water to Facilitate Organic Aerosol Formation: Assessing Knowledge

588 Gaps about Precursors and Partitioning, Environ. Sci. Technol., 51, 3327-3335,
589 https://doi.org/10.1021/acs.est.6b04540, 2017.
590 Sato, K., Hatakeyama, S., and Imamura, T.: Secondary organic aerosol formation during the
591 photooxidation of toluene: NOx dependence of chemical composition, J. Phys. Chem.
592 A, 111, 9796-9808, https://doi.org/10.1021/jp071419f, 2007.
593 Seinfeld, J. H.; Pandis, S. N. Atmospheric Chemistry and Physics:From Air Pollution to
594 Climate Change, 2nd ed.; Wiley: Hoboken, NJ, 2006.
595 Smith, M. L., Kuwata, M., and Martin, S. T.: Secondary Organic Material Produced by the
596 Dark Ozonolysis of α-Pinene Minimally Affects the Deliquescence and Efflorescence
597 of Ammonium Sulfate, Aerosol Sci. Tech., 45, 244-261,
598 https://doi.org/10.1080/02786826.2010.532178, 2011.
599 Smith, M. L., Bertram, A. K., and Martin, S. T.: Deliquescence, efflorescence, and phase
600 miscibility of mixed particles of ammonium sulfate and isoprene-derived secondary
601 organic material, Atmos. Chem. Phys., 12, 9613-9628, https://doi.org/10.5194/acp-
602 12-9613-2012, 2012.
603 Smith, M. L., You, Y., Kuwata, M., Bertram, A. K., and Martin, S. T.: Phase Transitions and
604 Phase Miscibility of Mixed Particles of Ammonium Sulfate, Toluene-Derived
605 Secondary Organic Material, and Water, J. Phys. Chem. A, 117, 8895-8906,
606 https://doi.org/10.1021/jp405095e, 2013.
607 Song, M., Liu, P. F., Hanna, S. J., Zaveri, R. A., Potter, K., You, Y., Martin, S. T., and
608 Bertram, A. K.: Relative humidity-dependent viscosity of secondary organic material
609 from toluene photo-oxidation and possible implications for organic particulate matter
610 over megacities, Atmos. Chem. Phys., 16, 8817-8830, https://doi.org/10.5194/acp-16-
611 8817-2016, 2016.
612 Takahama, S., Pathak, R. K., and Pandis, S. N.: Efflorescence Transitions of Ammonium
613 Sulfate Particles Coated with Secondary Organic Aerosol, Environ. Sci. Technol., 41,
614 2289-2295, https://doi.org/10.1021/es0619915, 2007.
615 Volkamer, R., Jimenez, J. L., San Martini, F., Dzepina, K., Zhang, Q., Salcedo, D., Molina, L.
616 T., Worsnop, D. R., and Molina, M. J.: Secondary organic aerosol formation from
617 anthropogenic air pollution: Rapid and higher than expected, Geophys. Res. Lett., 33,
618 L17811, https://doi.org/10.1029/2006gl026899, 2006.
619 Wong, J. P. S., Lee, A. K. Y., and Abbatt, J. P. D.: Impacts of Sulfate Seed Acidity and Water
620 Content on Isoprene Secondary Organic Aerosol Formation, Environ. Sci. Technol.,
621 49, 13215-13221, https://doi.org/10.1021/acs.est.5b02686, 2015.
622 Zhang, X., Cappa, C. D., Jathar, S. H., McVay, R. C., Ensberg, J. J., Kleeman, M. J., and
623 Seinfeld, J. H.: Influence of vapor wall loss in laboratory chambers on yields of
624 secondary organic aerosol, P. Natl. Acad. Sci., 111, 5802-5807,
625 https://doi.org/10.1073/pnas.1404727111, 2014.
626 Zhang, X., Schwantes, R. H., McVay, R. C., Lignell, H., Coggon, M. M., Flagan, R. C., and
627 Seinfeld, J. H.: Vapor wall deposition in Teflon chambers, Atmos. Chem. Phys., 15,
628 4197-4214, https://doi.org/10.5194/acp-15-4197-2015, 2015.
629 Zhang, Z., Zhang, Y., Wang, X., Lü, S., Huang, Z., Huang, X., Yang, W., Wang, Y., and
630 Zhang, Q.: Spatiotemporal patterns and source implications of aromatic hydrocarbons

631 at six rural sites across China's developed coastal regions, J. Geophys. Res.-Atmos.,
632 121, 2016JD025115, https://doi.org/10.1002/2016JD025115, 2016.
633 Zhao, Y., Saleh, R., Saliba, G., Presto, A. A., Gordon, T. D., Drozd, G. T., Goldstein, A. H.,
634 Donahue, N. M., and Robinson, A. L.: Reducing secondary organic aerosol formation
635 from gasoline vehicle exhaust, P. Natl. Acad. Sci., 114, 6984-6989,
636 https://doi.org/10.1073/pnas.1620911114, 2017.
637

Atmos. Chem. Phys. Discuss., https://doi.org/10.5194/acp-2017-1008
Manuscript under review for journal Atmos. Chem. Phys.
Discussion started: 8 November 2017


Atmospheric Chemistry and Physics Discussions

638

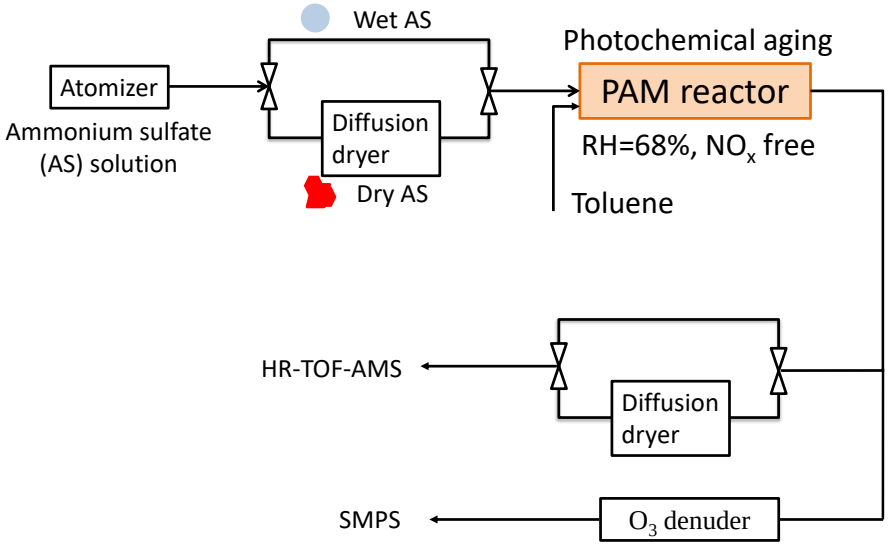


639

640 **Fig. 1.** Schematic of the experimental setup. The aqueous ammonium sulfate (AS) seed
641 particles either passed through a diffusion dryer so that the phase of the seed particles
642 could be altered or bypassed the diffusion dryer. Either wet or dry AS served as seed
643 particles for the experiments.

Atmos. Chem. Phys. Discuss., https://doi.org/10.5194/acp-2017-1008
Manuscript under review for journal Atmos. Chem. Phys.
Discussion started: 8 November 2017


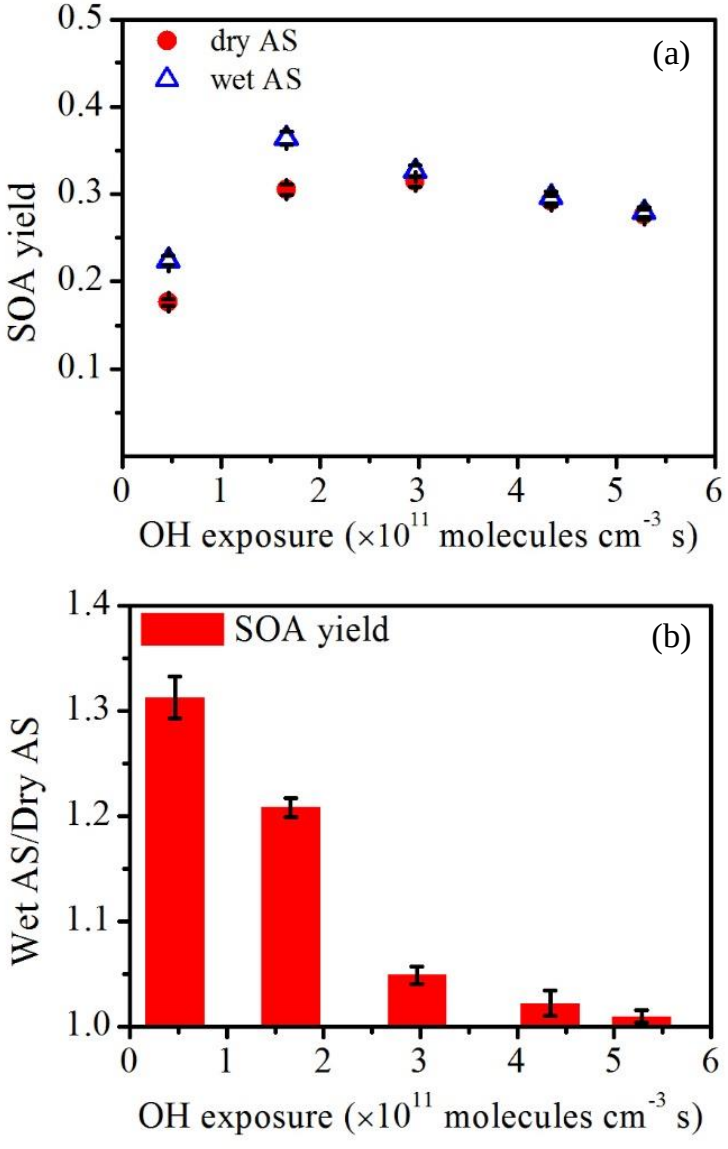


644

645 **Fig. 2.** (a) Yield of toluene-derived SOA formed on initially wet and dry AS as a
646 function of OH exposure. (b) Ratio of SOA yields on initially wet AS to those on
647 initially dry AS as a function of OH exposure.

648

Atmos. Chem. Phys. Discuss., https://doi.org/10.5194/acp-2017-1008
Manuscript under review for journal Atmos. Chem. Phys.
Discussion started: 8 November 2017


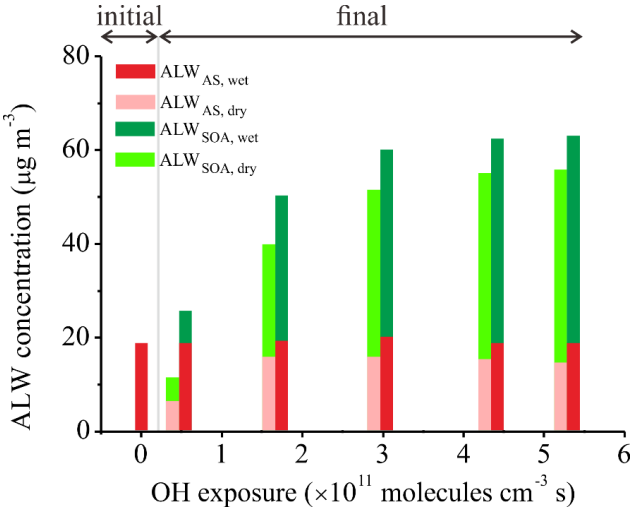


649

650 **Fig. 3.** Mass concentration of ALW uptake by AS and toluene-derived SOA before

651 (initial) and after reactions (final) for both initially wet and dry AS seeds. Adjoining

652 bars for initially wet and dry seeds have same OH exposures.

653

Atmos. Chem. Phys. Discuss., https://doi.org/10.5194/acp-2017-1008
Manuscript under review for journal Atmos. Chem. Phys.
Discussion started: 8 November 2017


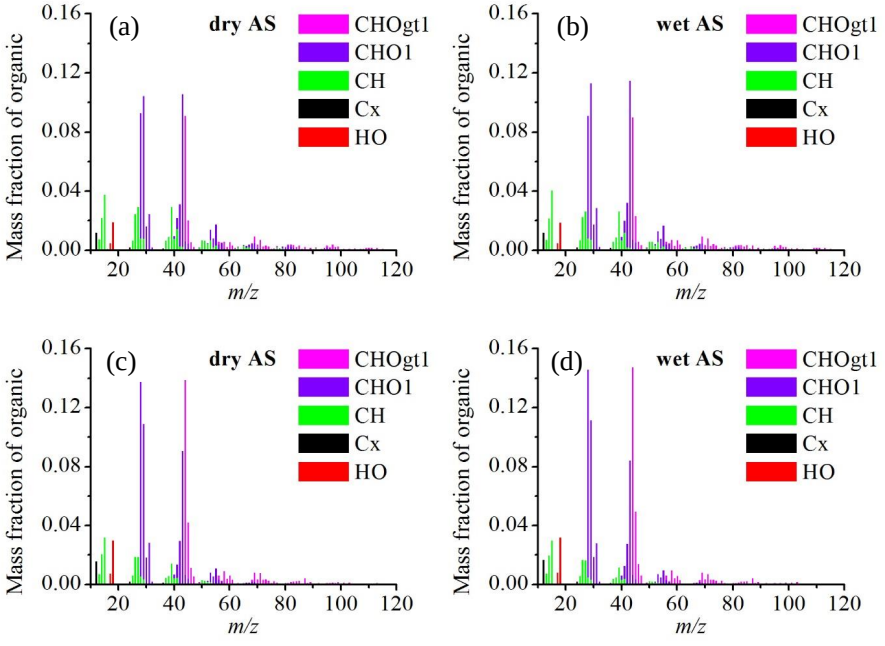


654

655 **Fig. 4.** High-resolution mass spectra of toluene-derived SOA on initially wet and dry

656 AS at an OH exposure of (a, b) $4.66\times10^{10}$ molecules $cm^{-3}$ s and (c, d) $5.28\times10^{11}$

657 molecules $cm^{-3}$ s.

Atmos. Chem. Phys. Discuss., https://doi.org/10.5194/acp-2017-1008
Manuscript under review for journal Atmos. Chem. Phys.
Discussion started: 8 November 2017


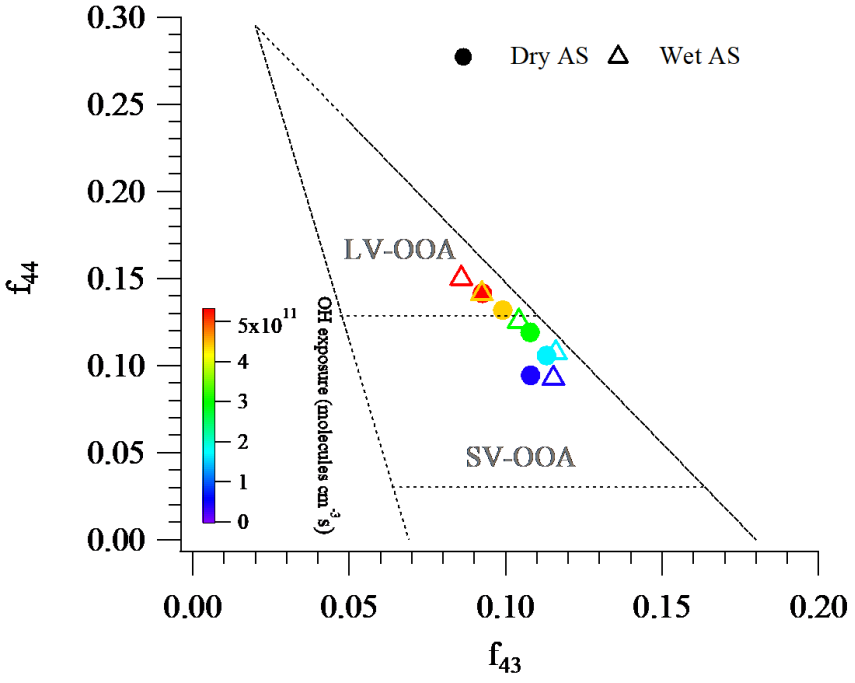


**Fig. 5.** Fractions of total organic signal at *m/z* 43 ($f_{43}$) vs. *m/z* 44 ($f_{44}$) from SOA data obtained in this study together with the triangle plot of Ng et al. (2010). Ambient SV–OOA and LV–OOA regions are adapted from Ng et al. (2010). Data are colored according to the OH exposure.

Atmos. Chem. Phys. Discuss., https://doi.org/10.5194/acp-2017-1008
Manuscript under review for journal Atmos. Chem. Phys.
Discussion started: 8 November 2017


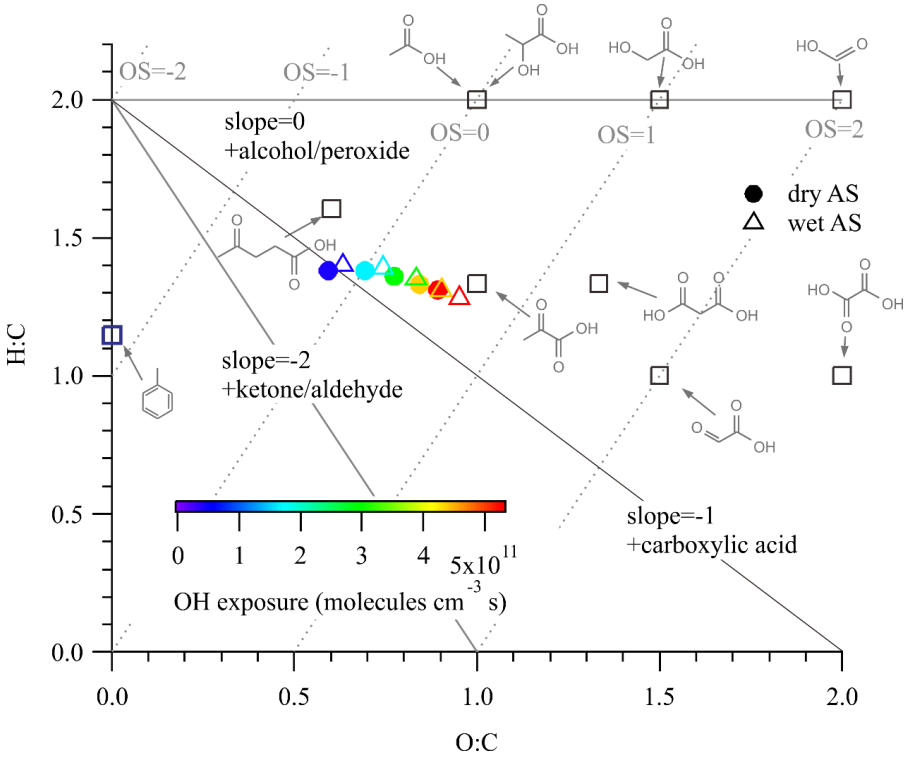


**Fig. 6.** Van Krevelen diagram of SOA derived from the photooxidation of toluene on initially wet and dry AS seed particles. SOA data are colored according to the OH exposure. Products identified in toluene-derived SOA are shown in boxes (Bloss et al., 2005; Hamilton et al., 2005; Sato et al., 2007). Average carbon oxidation states from Kroll et al. (2011) and functionalization slopes from Heald et al. (2010) are shown for reference.